Implantable Neuroamplifers for Electrocorticography Using Flexible and Biocompatible Technology

Juan Pablo Marcoleta,* Waldo Nogueira, Néstor Becerra Yoma, Jorge Wuth, Filip Jakimovski, Victor M. Fuenzalida, and Theodor Doll*

Brain signals such as electroencephalography (EEG) and electrocorticography (ECoG) are used to diagnose epilepsy. ECoG signals are small and therefore require large amplification while keeping the recording electronics small enough to adapt to the surface of the brain. Moreover, the components have to be of low power to reduce the risk of brain damage while recording the brain. Herein, a neuroamplifier that is integrated in an ECoG is described. The amplifier, in combination with a novel multiplexing system that reduces the number of required amplifiers and ensures the flexibility of the ECoG, achieves the desired signal-to-noise ratio while reducing power consumption. The feasibility of the proposed design is validated though electronic simulations for different input signals, analyzing the actual amplification achieved and the response times. Moreover the circuit is implemented and real measurements are provided validating the simulations.

1. Introduction

Electronic systems are increasingly influential in medicine, from monitoring systems to telemedicine.[1] The complexity and functionality of new electronic chips have increased, reducing the physical dimensions as predicted by Moore's law.[2] It is possible to use electronic implant systems to help diagnose neurological diseases.[3] Brain signals such as electroencephalography (EEG) and electrocorticography (ECoG) are used to diagnose epilepsy[4] and have a very low amplitude between 1 μV and 5 mV. Other biological signals like ECG and electromyography have an amplitude that ranges from 100 μV to 5 mV.[5,6] These waveforms need amplification before being processed by an analogue digital converter (ADC). The use of neuronal signals has a great impact

on the restoration of the lost function of people with disabilities. For example, Utah electrode array can capture brain signals and control a robotic arm.[7–9]

ECoG signals, as mentioned earlier, are used for the diagnosis of epilepsy. Some studies aim to show that it is possible to control a cursor with an ECoG array placed in the sensorimotor cortex.[10] In addition, research shows that it is possible to improve the waveform resolution using micro-ECoG, thereby improving the accuracy of the brain signals captured to decode finger movements.[11] These potential uses of ECoG lead to the development of implantable devices to restore lost function in people with disabilities.[12] Nevertheless, implantable devices must be encapsulated using biocompatible materials, not only to protect electronics from external fluids, but also to make these devices implantable as pacemakers and cochlear implants.[13,14] The materials and process that can be used to encapsulate the ECoG will be discussed in the following sections.

In the case of using ECoG to read neurological signals, it is required that the electronic systems to be implanted must be small enough to adapt to the surface of the brain.[15] In addition, the components should not exceed a power consumption of 40 mW cm^{-2} because they could cause damage to the brain.[16] These measured signals need amplification and this research aims to develop a neuroamplifier that can be integrated directly into the ECoG, which in turn improves the signal-to-noise ratio (SNR). In addition, energy consumption can be reduced by combining this amplifier with a multiplexing system that reduces

J. P. Marcoleta, Prof. W. Nogueira, F. Jakimovski, Prof. T. Doll
Department of Otolaryngology
Cluster of Excellence "Hearing4all"
Hannover Medical School
Hannover, Germany
E-mail: marcoleta.juan@mhh-hannover.de; theodoll@web.de

The ORCID identification number(s) for the author(s) of this article can be found under https://doi.org/10.1002/pssa.201900830.

Prof. N. B. Yoma, J. Wuth
Speech Processing and Transmission Laboratory
Department of Electrical Engineering
University of Chile
Santiago, Chile

Prof. V. M. Fuenzalida
Departamento de Fisica
Facultad de Ciencias Físicas y Matemáticas
Universidad de Chile
Av. Beauchef 850, Santiago, Chile

Prof. T. Doll
Biomaterial Engineering
Fraunhofer Institute of Toxicology and Experimental Medicine ITEM
Hannover, Germany

**ADVANCED
SCIENCE NEWS**

www.advancedsciencenews.com

pss
physica status solidi a

www.pss-a.com

the amount of amplifiers required, thus ensuring the flexibility of the ECoG array.[17] As far as the authors know, this type of solution is not found in the specialized literature.

The rest of the manuscript is divided as follows: in the experimental section, we discuss the state of the art of neuroamplifiers, the configuration to carry out measurements, biomaterials, and the process to encapsulate electronics. Solutions are also proposed to reduce parasitic capacitances and dimension the required bandwidth of the operational amplifiers. In the results section, simulated and electronically implemented measurements are presented. In the discussion section the results obtained with simulations and electronic implementation are compared regarding bandwidth and power consumption. The conclusion provides the final remarks and proposes future developments.

2. Experimental Section

This system aims to reduce energy consumption and ensure the flexibility of the ECoG, so the dimensions and number of electronic components should be as small as possible. This was achieved by integrating the amplification device into a multiplexer system to reduce the amount of amplifiers used. This section will discuss the characteristics of these amplifiers, the parasitic elements, the bandwidth requirements of the operational amplifier, the biomaterials used, and the process to encapsulate the electronics.

2.1. Amplifiers

EEG signals such as ECoG signals need differential amplifiers that amplify the difference in voltage between two electrodes.[1] Due to the low voltage measured from the recording surface electrodes, i.e., around 5–100 μV,[18] they usually require an amplification of around 40–60 dB and a bandwidth between 1 Hz and 10 kHz.[19] This amplifier was combined with a multiplexing system to reduce the amount of amplifiers needed, so that the power consumption was less than 40 mW cm^{-2} and the amount of cables to transmit the signals to an external device was low, increasing the flexibility of the ECoG matrix.

The gain bandwidth product (GBP) of the operational amplifiers must be sized so as to be able to represent the multiplexed signals of several ECoG sensors with the least possible error. However, the higher the GBP, the greater the power consumption of the operational amplifier. These amplifiers were the front ends of the system, that is, they were integrated into the ECoG. The output of each of these amplifiers will be the input of a differential amplifier that will be external to the ECoG, i.e., back end (**Figure 1**).

2.2. Electronic Setup

Because the amplifier is close to the signal source (the electrode) and the noise is lower, it is possible to ensure a high SNR. The back end does not need a high amplification because this is performed on the front-end amplifiers.

The test signals were generated electronically and measured by an oscilloscope. These signals were sampled, multiplexed, amplified, and analyzed using MATLAB (Mathworks, Massachusetts, USA) and Proteus (Labcenter, North Yorkshire, England). The amplification was estimated, the signals were plotted, and the energy consumption density of this system was calculated, which must be less than 40 mWcm^{-2}. **Figure 2** shows the electronic scheme for five constant inputs.

2.3. Parasitic Elements

In the solution presented here, parasitic elements were produced due to spurious capacitance and resistance in the operational amplifier,[21,22] the CMOS switches, and cables. These CMOS switches were in parallel, and the total parasitic capacitance depends on the number (N) of CMOS switches multiplied by the internal CMOS capacitance (Cswitch) plus the internal input capacitance of the amplifier (Camp), as expressed in Equation (1).

$$C_{\text{total}} = N \cdot C_{\text{switch}} + C_{\text{amp}} \tag{1}$$

The internal capacitance of the amplifier was lower compared with the capacitance of the switches so it was discarded.
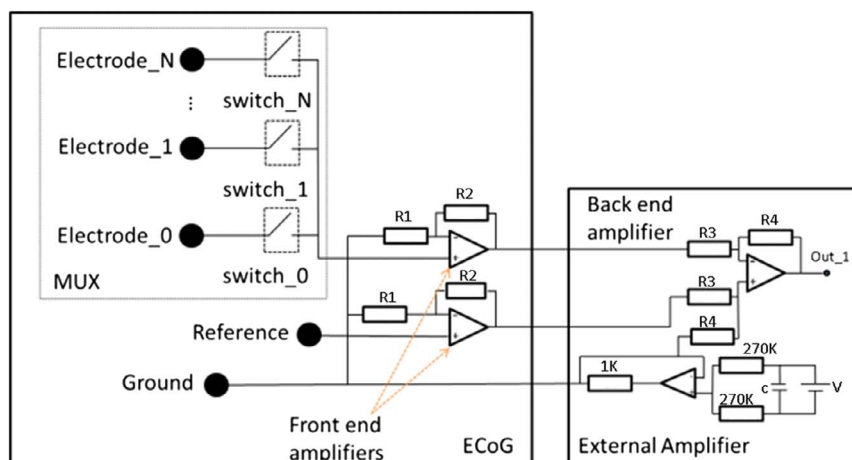
Figure 1. Amplifier circuit. The pulses from the multiplexed signals are preamplified and amplified by the front-end and differential back-end amplifiers, respectively. The resulting signal is denoted as Out_1. Ground corresponds to a virtual one implemented with an amplifier configuration similar to those used elsewhere.[20]
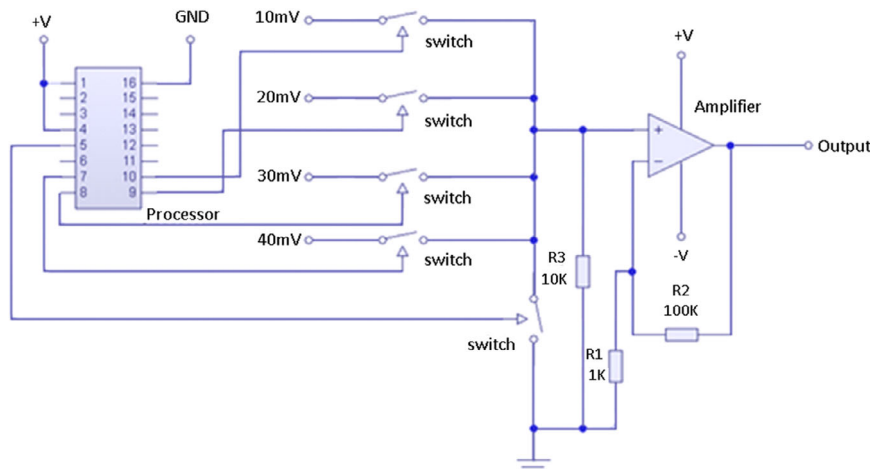
Figure 2. The front-end amplifier and the multiplexed input signals. The processor controls the CMOS switches that sample the input signals, which are amplified. After sampling a given input signal, the CMOS switch is activated to discharge the corresponding CMOS capacitance.

Figure 3. Schematic of parasitic elements for one channel: Rwire, wire resistance; Cwire, wire capacitance; Cswitch, switch capacitance; and, Camp, amplifier resistance.

To compensate for this capacitive effect, the grounded CMOS switch in Figure 2 was used. The circuit of equivalent parasitic elements is shown in **Figure 3**.

2.4. The Gain Bandwidth Product

Each input waveform that was sampled was represented with pulse amplitude modulation (PAM) in the multiplexed signal. The sampling frequency, the PAM pulse duration, and the number of multiplexed channels determined a requirement for the bandwidth of the front-end amplifier. However, each type of operational amplifier had a GBP. In addition, the consumption of the operational amplifier depended on GBP. To assess the effect of GBP on the viability of the proposed solution, simulations with Proteus (Labcenter Electronics Ltd, Skipton United Kingdom)[23–25] and an electronic implementation were used to calculate the relative percentage error between the theoretical gain (G_0) and that obtained. The theoretical gain corresponded to the R_2/R_1 ratio in Figure 2 and was compared with the measured value of the maximal signal gain of simulation and implementation (G_m). The percentage relative error (Err(%)) was calculated as

$$\text{Err}(\%) = \frac{G_0 - G_m}{G_0} \times 100 \qquad (2)$$

This percentage error was evaluated for 11 amplifiers with different GBP using Proteus. Next, five amplifiers with GBP similar to those that gave the best results with the Proteus simulation were tested in the electronic implementation. Each

channel was sampled at a constant rate of 10 KSamples s^{-1}. As five channels were used the total sampling frequency was 50 KSamples s^{-1}. The front-end amplifier had an amplification of 40 dB.

2.5. Biocompatibility

To make the system implantable and therefore biocompatible, it is necessary to encapsulate the electronic components—not only to make the system biocompatible, but also to protect the electronic components from body fluids. It is possible to do it using a 3D printing process, to print the pathway using graphene ink that connects the components and can then be encapsulated using polydimethylsiloxan (PDMS),[26] as it is standard for some implantable devices.[13] Its surface composition was studied with respect to the etching condition using X-ray photoelectron spectroscopy.[27] This encapsulation was obtained, as shown in **Figure 4**.

3. Results

This section will present the measurements of the percentual gain error, graphs of the amplified multiplexed waveform for different input signals that were kept constant, response time of the amplifier, and energy consumption. The results obtained with the simulation and with the electronic implementation are shown in Sections 3.1 and 3.2, respectively.

1900830 (3 of 7)
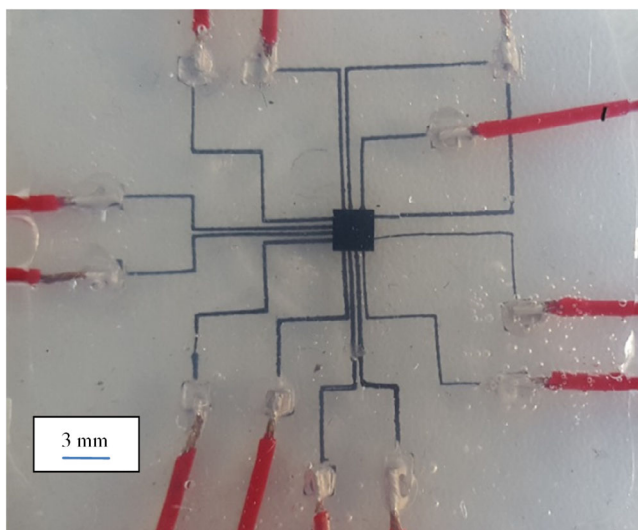
Figure 4. Chip encapsulation with PDMS and wiring using graphene ink.

Table 1. Simulated with Proteus, GBP, theoretical gain, relative error, and response time for different amplifiers.

Amplifier	GBP [kHz]	Theoretical gain (G_0)	Measured gain (G_m)	Err (%)	Response time [µs]
ADA4505	50	100	5	95	6
AD8607	400	100	7.5	92	6
741	1000	100	25	75	6
TL082	4000	100	75	25	6
AD797	8000	100	100	15	0.2
AD8671	10 000	100	100	10	2.5
Op37	12 000	100	100	4	1
AD745	20 000	100	100	0	1
AD817	50 000	100	100	0	1
HA5221	100 000	100	100	0	0.5
AD8040	125 000	100	100	0	0.5
Opa355	200 000	100	100	0	0.1
AD8055	300 000	100	100	0	0.1

3.1. Simulated Results

Table 1 shows GBP, G_0, G_m, and relative gain error. In this section, the results of gain, response time, and relative error for the simulated circuit will be presented. As mentioned earlier, the proposed circuit was simulated with Proteus. No special setup is needed. The simulation included the 16F1503 microcontroller, TS5A3157 CMOS switches, and the amplifiers shown in Table 1.

As shown in Table 1, a higher GBP leads to a lower relative gain error and response time with the multiplexed input signal. However, another important parameter is the "slew rate." For example, the AD797 amplifier has a GBP around 12 times lower than the HA5221, but both yielded a similar response time. The electronic evaluation circuit was implemented with amplifier GBPs greater than 4 MHz for the multiplexed input signal described here. **Table 2** shows the input waveform and the

Table 2. Results for electronic simulation.

Signal	Graphic	Err (%)
Input signal		
Output: Tl082		25
Output: Op37		4
Output: AD745		≅0
Output: HA5221		≅0
Output: opa355		≅0

corresponding amplified output for five operational amplifiers with GBP equal to 4, 8, 12, 20, and 200 MHz, respectively. **Table 3** shows the input waveform and the corresponding amplified output for operational amplifiers with the same GBP using the electronic setup.
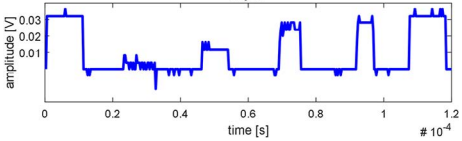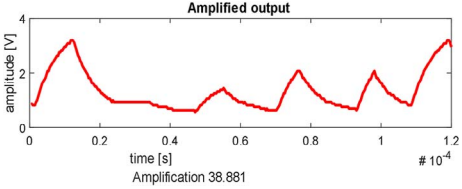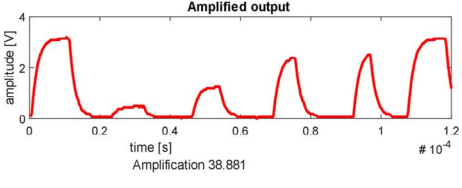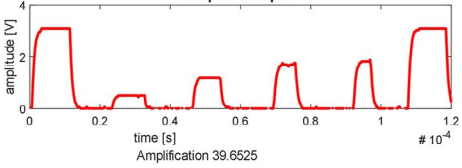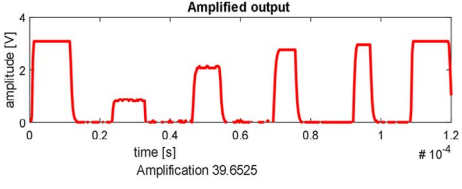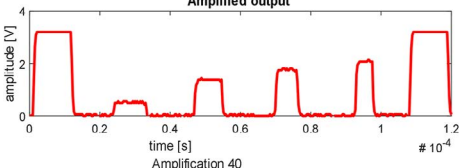
3.1.1. Energy Consumption

Table 4 shows the energy consumption for the amplifiers evaluated by simulation according to Table 1. The minimum operating voltage according to the manufacturer was used.

Table 4 shows that in general the power densities are higher as the GBP increases and the package surface decreases. A larger package naturally reduces energy density but impairs the flexibility of the ECoG. For example, the AD8040 amplifier has a GBP of 125 MHz, and with a 5 × 6 mm package, it is possible, from an energy density point of view, to be used as an implantable system. However, if the package is reduced to 1.25 mm × 2 mm,

Table 3. Results for electronic implementation.

Amplifier	Signal	Err (%)
Input		
TL082		12.09
NJM2100		12.09
OPA322		3.92
AD8072		3.92
NJM2137		≅0

to increase the flexibility of the ECoG, the energy density is increased to 48 mWcm^{-2}. At this point, it is worth highlighting that the amplifier design needs a compromise between, GBP, power consumption, chip size, maximum voltage, response time, and the relative gain error obtained.

3.2. Electronic Implementation

The following section shows the amplification results obtained with the multiplexed input signal using electronic implementation. In addition, the energy consumption density is estimated, using the information given by the manufacturer. This implementation was conducted using a protoboard. It should be considered that the system was exposed to environment noise,

which influenced the measurements. The cables were short but their diameter was not much wider than one of the ECoG cables, which is typically 50–100 μm.[28] In the case of the cables used in the protoboard, the diameter was about 600 μm. Consequently, the testing condition could not be considered ideal when compared with the real operating scenario.

3.2.1. Amplification and Response Time

This section shows the amplified waveform, the amplification relative error (Err(%)), and the response time obtained with the electronic circuit.

These results show that there is a capacitive effect observed with those amplifiers that provide the lowest GBPs. It can be highlighted that this effect reduces as the GBP increases. This can be quantified by the reduction of Err(%) when GBP increases. It is important to mention that the measure of the input and output amplitudes can be interfered by electrical noise, which in turn can also affect Err(%). To avoid or reduce this effect, Err(%) was estimated using the maximal amplitude of the input and output signals.

3.2.2. Energy Consumption

The power consumption was measured in the conditions that generated the signals shown in Section 3.2.1 (see **Table 5**). It is possible to reduce these voltages and the power consumption of the amplifiers, as specified by the manufacturer's data sheet (see **Table 6**). However, it would be necessary to adjust the gain of each amplifier, which was not performed in the tests because the gain was kept constant. In the laboratory tests, dual in-line package was used to facilitate the manipulation of the chips. However, smaller packages were considered in the energy density estimation based on the manufacturer's data. We considered for our electronic implementation a subset of the amplifiers shown in Table 1 that could provide a wide range of GBP.

4. Discussion

This work proposes an amplifier system that can be integrated into an ECoG to amplify the weak signals that come from the electrodes. The amplifier input corresponds to the multiplexed waveforms from a given number of electrodes. This multiplexing is performed using CMOS switches activated by a microcontroller. All electronics are integrated in the ECoG using biocompatible technology to encapsulate the electronic system to be implantable and protect it from fluids that come from the brain. The results show that the overall sampling frequency of the input multiplexed signal conditions the amplifier GBP. It was observed that there is a capacitive effect that decreases when GBP increases. The evaluations conducted here suggest that for a signal with a total sampling frequency of 50 kSamples s^{-1}, which corresponds to five electrodes sampled with a PAM signal at 10 kSamples s^{-1} and an amplification of 40 dB, a GBP greater or equal to 8 MHz is required. This analysis considered the percentage error of simulated gain equal to zero compared with the theoretical gain, i.e., 40 dB.

Table 4. Simulated power consumption for the amplifiers shown in Table 1.

Amplifier	Current [mA]	Voltage [±V]	Power Consumption [mW]	Minimal Package area [mm²]	Power density [mW cm⁻²]	Maximal package area [mm²]	Power density [mW cm⁻²]
ADA4505	0.15	2.0	0.60	1.2	48	32	1.8
AD8607	0.10	2.0	0.40	8.1	4.9	33	1.2
741	0.020	2.0	0.080	58	0.14	82	0.090
TL082	1.4	4.0	11	33	34	14×10^2	8.3
AD797	8.0	2.0	32	20	16×10^2	59	55
AD8671	2.0	4.0	16	9.0	18×10^2	35	46
Op37	3.8	4.0	30	20	15×10^2	67	45
AD745	10	2.0	40	76	53	76	53
HA5221	9.0	4.0	72	20	36×10^2	81	89
AD8040	0.30	2.0	1.2	2.5	48	30	4.0
Opa355	8.0	2.0	32	4.6	69×10^2	4.6	69×10^2
AD8055	5.0	2.0	20	4.6	43×10^2	20	10×10^2

Table 5. Consumption and density of energy consumption for the different amplifiers evaluated in the electronic circuit.

Amplifier	Current [mA]	Voltage [±V]	Power consumption [mW]	Minimal package area [mm²]	Power density [mW cm⁻²]
TL082	3.8	4.0	30	70	43
NJM2100	5.1	4.0	41	56	73
opa320	2.0	4.0	16	4.6	35
AD8072	6.1	3.0	37	70	52
NJM2137	1.1	2.0	4.4	56	7.9

Table 6. Estimation of consumption and energy consumption density for the family of amplifiers tested with the electronic circuit based on the data provided by the manufacturer.

Amplifier	Current [mA]	Voltage [±V]	Power consumption [mW]	Minimal package area [mm²]	Power density [mW cm⁻²]
TL082	1.4	5.0	14	13	11×10^2
NJM2100	3.5	1.0	7.0	20	35
opa320	1.5	1.8	5.4	19	28
AD8072	5.0	2.5	25	20	13×10^2
NJM2136	0.6	1.4	1.7	19	8.9

In addition, it is shown that in general amplifiers with a higher GBP have a higher energy consumption. The power consumption of amplifiers such as AD745 or AD8055 is up to the limit of 40 mW cm⁻², where necrosis can occur in the brain. In contrast, the NJM 2137 amplifier requires 4 mW cm⁻² under the conditions provided by the manufacturer and the considered encapsulation. Therefore, this amplifier is safe to be implanted in the ECoG because the power consumption density is less than the upper bound of 40 mW cm⁻². The bibliography considers the power density of implanted electronics. However, Reichert[16] presented a model of an implantable device with a power density higher than 40 mW cm⁻¹ that can produce a dangerous increase in temperature equal to 2 °C. It is important to mention that the design of this amplifier requires a compromise between chip size, power consumption, and stabilization time. In our case, the ideal signal amplification with the lowest energy consumption was achieved with NJM2137 with electronic implementation.

In the case of electronic implementation, it is also shown that a higher GBP generally requires a higher energy consumption, but it is possible to energize the amplifier with a lower voltage and reduce the power consumption of the amplifier. It is important to note that in the case that the amplifier is energized with positive voltage, the energy consumption can be reduced, but the input signal must be positive. To achieve this, it is necessary to use a voltage divider.

5. Conclusion

This work proposed an amplifier circuit that can be integrated into an ECoG array to be implanted using 3D printing techniques. The presented solution multiplexes a given number of input electrodes, whose waveforms are sampled using PAM. GBP and energy consumption density were evaluated to amplify the multiplexed input, whose input frequency is 50 kSamples s⁻¹, corresponding to five channels, by 40 dB. For this purpose, simulations were conducted using Proteus of 11 amplifiers and a subset of five of these was tested with an electronic circuit. The relative error between the theoretical and the obtained amplification gain and the response time were used as comparison criteria. Another important aspect considered was the dimension of the package that has a direct impact on power consumption density. The minimum GBP for the multiplexed input signal and the specified gain was estimated at 8 MHz. Amplifiers op320 and NJM2137 can meet the conditions of GBP, and maximum power consumption density was

identified. The proposed solution ensures the flexibility of the ECoG array by reducing the number of chips and the amount wires and keeping the power consumption density under control.

Conflict of Interest

The authors declare no conflict of interest.

[1] *Handbook of Medical Technology* (Eds: R. Kramme, K. P. Hoffmann, R. Pozos), Springer-Verlag, Heidelberg, Germany **2011**.

[2] G. E. Moore, *IEEE Solid-State Circuits Soc. Newsl.* **2006**, *11*, 33.

[3] J. P. Marcoleta, W. Nogueira, U. P. Froriep, T. Doll, *Phys. Status Solidi A* **2018**, *215*, 1700134.

[4] A. Sotelo, E. Guijarro, L. Trujillo, L. N. Coria, Y. Martínez, *Comput. Biol. Med.* **2013**, *43*, 1713.

[5] X. Yang, J. Hu, Z. Chen, H. Yang, An 8-Channel General-Purpose Analog Front-End for Biopotential Signal Measurement, https://www.semanticscholar.org/paper/An-8-Channel-General-Purpose-Analog-Front-End-for-Yang-Hu/920024e246e19f86e5e5dde94c3e296d7fd5660c (accessed: September 2019).

[6] K. Ito, T. Tani, T. Iwagami, S. Nishino, K. Kiyoyama, T. Tanaka, *Electron. Comm. Jpn.* **2018**, *101*, 47.

[7] C. E. Bouton, A. Shaikhouni, N. V. Annetta, M. A. Bockbrader, D. A. Friedenberg, D. M. Nielson, G. Sharma, P. B. Sederberg, B. C. Glenn, W. J. Mysiw, A. G. Morgan, *Nature* **2016**, *533*, 247.

[8] G. Sharma, D. A. Friedenberg, N. Annetta, B. Glenn, M. Bockbrader, C. Majstorovic, S. Domas, W. J. Mysiw, A. Rezai, C. Bouton, *Sci. Rep.* **2016**, *6*, 33807.

[9] J. L. Collinger, B. Wodlinger, J. E. Downey, W. Wang, E. C. Tyler-Kabara, D. J. Weber, A. J. McMorland, M. Velliste, M. L. Boninger, A. B. Schwartz, *Lancet* **2013**, *381*, 557.

[10] W. Wang, J. L. Collinger, A. D. Degenhart, E. C. Tyler-Kabara, A. B. Schwartz, D. W. Moran, D. J. Weber, B. Wodlinger, R. K. Vinjamuri, R. C. Ashmore, J. W. Kelly, *PLoS One* **2013**, *8*, e55344.

[11] W. Wang, A. D. Degenhart, J. L. Collinger, R. Vinjamuri, G. P. Sudre, P. D. Adelson, D. L. Holder, E. C. Leuthardt, D. W. Moran, M. L. Boninger, A. B. Schwartz, D. J. Crammond, E. C. Tyler-Kabara, D. J. Weber, in *Proc. 31st Annual Int. Conf. of the IEEE Engineering in Medicine and Biology Society*, IEEE, Minneapolis, MN **2009**, pp. 586–589.

[12] M. J. Vansteensel, E. G. Pels, M. G. Bleichner, M. P. Branco, T. Denison, Z. V. Freudenburg, P. Gosselaar, S. Leinders, T. H. Ottens, M. A. Van Den Boom, P. C. Van Rijen, *N. Engl. J. Med.* **2016**, *375*, 2060.

[13] A. J. Teo, A. Mishra, I. Park, Y. J. Kim, W. T. Park, Y. J. Yoon, *ACS Biomater. Sci. Eng.* **2016**, *2*, 454.

[14] F. G. Zeng, *Trends Amplif.* **2004**, *8*, 1.

[15] A. Campbell, C. Wu, *Micromachines* **2018**, *9*, 430.

[16] *Indwelling Neural Implants: Strategies for Contending With the in Vivo Environment* (Ed: W. M. Reichert), CRC Press, Boca Raton, FL **2007**.

[17] M. Insanally, M. Trumpis, C. Wang, C. H. Chiang, V. Woods, K. Palopoli-Trojani, S. Bossi, R. C. Froemke, J. Viventi, *J. Neural Eng.* **2016**, *13*, 026030.

[18] G. Schalk, *Front. Neuroeng.* **2010**, *3*, 9.

[19] C. L. Kumaragamage, B. J. Lithgow, Z. Moussavi, *Biomed. Eng. Online* **2014**, *13*, 6.

[20] X. Chen, Z. J. Wang, presented at *5th Int. Conf. Bioinformatics and Biomedical Engineering*, Wuhan, May **2011**.

[21] A. Baht, Measure the Input Capacitance of an Op Amp, https://www.maximintegrated.com/en/design/technical-documents/app-notes/5/5086.html, (accessed: November 2019).

[22] M. Zaidi, I. Grout, A. K. bin A'ain, *Int. J. Electr. Comput. Energ. Electron. Comm. Eng.* **2017**, *11*, 239.

[23] E. García, *Compilador C CCS Y Simulador Proteus Para Microcontroladores PIC*, Marcombo, Mexico **2009**.

[24] M. P. Bates, *Programming 8-Bit microcontroller in C: With Interactive Hardware Simulation*, Elsevier/Newnes, Amsterdam **2008**.

[25] A. Singh, *Int. J. Adv. Res. Electr. Electron. Instrum. Eng.* **2015**, *4*, 9635.

[26] J. Stieghorst, A. Bondarenkova, N. Burblies, P. Behrens, T. Doll, *Biomed. Microdevices* **2015**, *17*, 54.

[27] V. Fuenzalida, T. Doll, presented at Int. Hear. Res. Closing the Aud. Efferent Loop, Valparaiso, Chile, March **2018**.

[28] B. Rubehn, P. Fries, T. Stieglitz, in *Proc. 4th European Conference of the International Federation for Medical and Biological Engineering* (Eds: J. Vander Sloten, P. Verdonck, M. Nyssen, J. Haueisen), Springer, Berlin, Heidelberg **2009**.